Inorganic Chemistry

Article

pubs.acs.org/IC

Building-up Remarkably Stable Magnesium Porphyrin Polymers Self-Assembled via Bidentate Axial Ligands: Synthesis, Structure, Surface Morphology, and Effect of Bridging Ligands

Sk Asif Ikbal, Sanfaori Brahma, and Sankar Prasad Rath*

Department of Chemistry, Indian Institute of Technology Kanpur, Kanpur-208016, India

Supporting Information

ABSTRACT: A series of supramolecular architectures of magnesium tetranitrooctaethylporphyrins mediated by several bidentate axial ligands have been synthesized in excellent yields and structurally characterized. Six conjugated axial ligand with increasing chain lengths have been utilized in the present investigations in which the Mg···Mg nonbonding distance between successive ions also increases from 0.73 to 2.70 nm in the series. To the best of our knowledge, this is the first report where stable metallo-porphyrin polymers with such long spacers have been synthesized in one pot so easily. Linear one-dimensional (1D) polymeric chains were observed in the X-ray structure of the six-coordinated complexes in which porphyrin units are aligned parallel to each other to have so-called "shish kebab" like architectures to maintain offset-stacked overlap. However, after an optimum Mg···Mg nonbonding distance, these 1D chain do not continue, rather they form five-coordinated porphyrin dimers with "wheel-and-axle" like architectures which are then self-aggregated by $\pi-\pi$ interactions in a perpendicular manner to fill space created by large bridging ligands more effectively which consequently results in spherical structures. The structures of the molecules in solution and their surface patterns on highly ordered pyrolytic graphite (HOPG) have also been investigated.

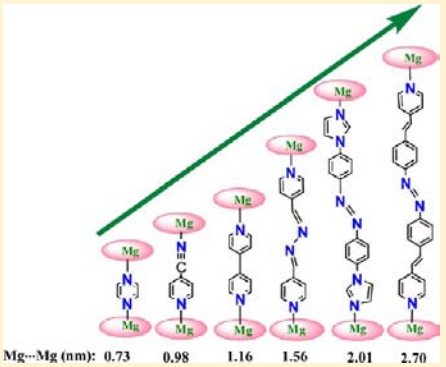

INTRODUCTION

Recently, multiporphyrin systems have drawn major attention for their structure-induced optical and electronic properties that have application in optical switches, conductive materials, and nonlinear optics.[1−10] Among them, a long and rigid porphyrin polymeric wire is of particular interest for preparation of next generation electronic devices.[10] In the biological systems, porphyrins and chlorophylls are often self-assembled into nanoscale superstructures to perform many essential functions, such as light harvesting and electron transport.[11] For example, the crystal structure of the light-harvesting (LH) antenna complex in purple photosynthetic bacteria shows the presence of a highly symmetric wheel-like supramolecular architecture involving a large number of bacteriochlorophyll pigments.[11e] As a mimic of the LH antenna complex, chemists have been trying to synthesize multiporphyrin arrays having structures like nanoring, nanofibers, nanorods, nanotubes, nanowires, and so forth.[12−18]

The applications of these supramolecular systems would require fabrication on substrate surfaces that are smooth at the molecular level.[12−18] Higher-order structures, such as wires, networks, and nanodots on surfaces are necessary for molecular electronic devices. Since porphyrins have tunable photophysical and chemical properties, the functionalities of their materials can be suitably manipulated. While many of the subtle mechanisms governing the aggregation of molecular species in solution have been unraveled, the understanding of the way the molecule comes together on the surfaces is still very limited.

While numerous multiporphyrin systems have been developed so far, most of them rely on rigid covalent linkages to achieve the shape persistent multiporphyrin structures.[6,7] Although rigid connections between porphyrin pigments are useful to materialize regular arrangement of porphyrins, the synthetic procedures become inevitably complicated, tedious, and also expensive. However, the preparation of supramolecular porphyrin polymers by self-assembly is intriguing since it involves a relatively light synthetic burden and tunability for length by control of external conditions. Hence, a supramolecular self-assembly system has become an attractive and alternative strategy to build well-ordered multiporphyrin arrays including models of light-harvesting antenna and long polymers for potential conductive wires and optical materials.[8−10] Among several other possible auxiliaries that can bind two or more metalloporphyrin units into a supramolecular aggregate, aliphatic and aromatic amines proved particularly useful as linkers. The metal ion and spacers provide additional variants of the supramolecular structure.

Although the abundance of chlorophyll and bactereochlorophyll is huge in nature, laboratory insertions of magnesium into porphyrinic compounds were difficult for quite some time.[19] It has been considerably more difficult to construct extended coordination polymers with the magnesium porphyrin building blocks, because of the flexible coordination

Received: April 23, 2012
Published: August 31, 2012

   dx.doi.org/10.1021/ic300826p | Inorg. Chem. 2012, 51, 9666−9676

numbers of magnesium ion and also its tendency to form a labile complex. Magnesium porphyrin is, however, quite stable in nonacidic solvent but rapidly demetalated under acidic conditions. There have been investigations on multiporphyrin coordination arrays based on magnesium porphyrin with combined electronic and photophysical study.[20] However, the stability of magnesium porphyrin has always been an issue.

Herein, we describe an unknown family of remarkably stable magnesium porphyrins which binds strongly with nearly linear, conjugated, and long axial ligands to generate long chains polymers. This objective has been achieved successfully by taking tetranitro octaethylporphyrins (*tn*-H_2OEP) as a porphyrin macrocycle. Ligands of varying length have been used as bridging auxiliaries between the metal centers, effecting heterogeneous porphyrin-ligand oligomeric as well as polymeric assemblies. The presence of four electron-withdrawing bulky nitro groups at the *meso* positions severely distorts the porphyrin geometry and provides an interesting modulation of the macrocycle properties which significantly enhanced the axial ligand affinity that enables the facile isolation of a series of infinite polymeric chains in solids with ease even under the offset effects of the macrocycle distortions. The structures of the molecules in solution and their surface pattern on highly ordered pyrolytic graphite (HOPG) have also been investigated.

RESULTS AND DISCUSSION

The free ligand (*tn*-H_2OEP) has been synthesized as reported previously,[21a] and the magnesium ion is inserted stirring the free ligand in dry dichloromethane with $MgBr_2{\cdot}O(Et)_2$ and triethylamine (few drops) under nitrogen for 1 h using a procedure reported[21b] for insertion of Mg ion in bisporphyrin which results in the isolation of dark green solid of Mg(*tn*-OEP) in excellent yields. The UV−vis spectrum of the molecule shows Soret and Q-bands at 431 and 570, 606 nm, respectively. Addition of excess axial ligand to magnesium tetranitrooctaethyl porphyrin in dichloromethane produce the monomeric complex in solution which upon spontaneous self-association readily produce polymeric chains in a single pot that leads to precipitation of the complex in pure crystalline form in excellent yields. Addition of excess pyrazine (L^1) into the dichloromethane solution of Mg(*tn*-OEP) (**1**) immediately results in red shifting of the Soret and Q bands which, after stirring in air at room temperature for 30 min, produce dark green precipitation that was isolated and characterized as $[Mg(tn\text{-}OEP)(pyrazine)]_n$, (**1**·$L^1$). Figure 1 represents the gradual changes in UV−visible spectra of Mg(*tn*-OEP) in presence of varying amounts of pyrazine (L^1) (host/guest ratio changes from 1:0.1 to 1:207) which shows the formation of

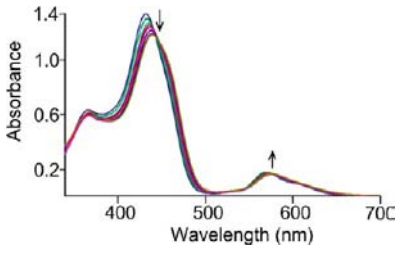

Figure 1. UV−vis spectral change (at 295 K) of **1** in dichloromethane upon addition of L^1 as the host:guest ratio changes from 1:0.1 to 1:207; arrows indicate increase or decrease of band intensity.

1·L^1. Similar observations are also obtained when other axial ligands (L^2 to L^6) are used. Here, no chromatographic or other tedious separation procedures are used. All the complexes have been isolated as solid just by filtration from the reaction mixture in excellent yields and structurally characterized except one (**1**·L^6) which however is geometrically optimized by using density functional theory (DFT). Scheme 1 shows the

Scheme 1

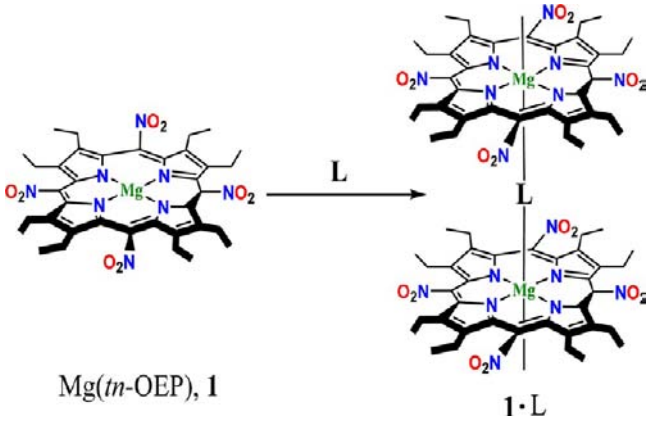

complexes and their abbreviations as reported in the present investigation while the axial ligands (L) used are of increasing lengths and are shown in Scheme 2. Synthetic procedure of the complexes and their spectral characterizations are given in detail in the Experimental Section.

Scheme 2

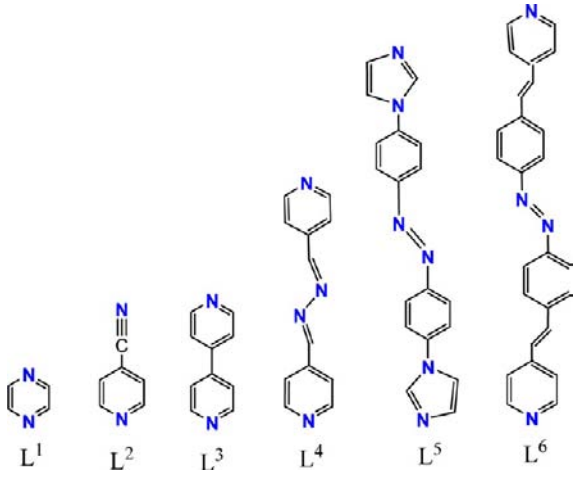

Crystallographic Characterizations. The molecules **1**·L^1 and **1**·L^4 crystallized in the orthorhombic crystal system while **1**·L^2, **1**·L^3 in the tetragonal system; Figures 2−5 illustrate the molecular packing which shows the formation of one-dimensional (1D) chains. Crystal data and data collection parameters are shown in Table 1 while selected bond distance and angles are reported in Table 2. Ligand L maintains nearly linear geometry which facilitates the formation of stable 1D polymeric chains with Mg(*tn*-OEP). The polymeric moieties maintain so-called "shish kebab" like architectures, the bridging bidentate ligand being aligned perpendicularly to the planes of the porphyrin units. The X-ray structures reveal that the Mg···Mg nonbonding distances between successive magnesium

dx.doi.org/10.1021/ic300826p | Inorg. Chem. 2012, 51, 9666−9676

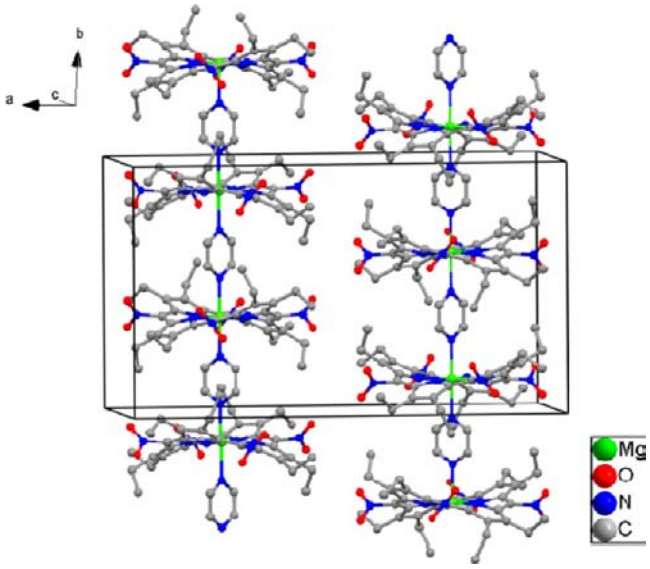

Figure 2. Diagram illustrating the packing of **1**·L^1 in the unit cell at 100 K (H-atoms and uncoordinated L^1 present in the crystal lattice have been omitted for clarity).

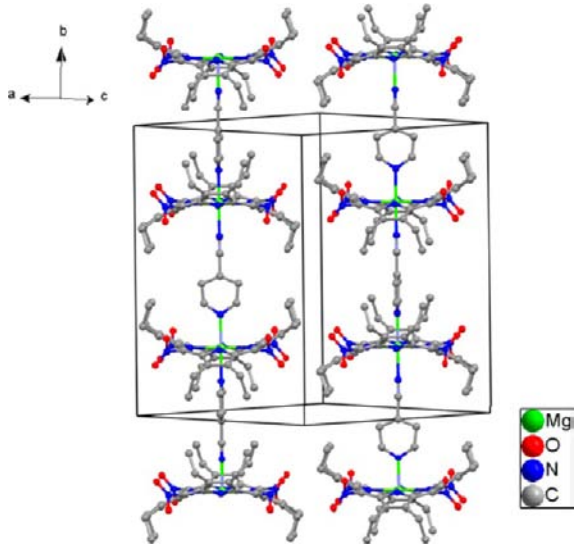

Figure 3. Diagram illustrating the packing of **1**·L^2 in the unit cell at 100 K [H-atoms and the uncoordinated solvent molecules (C_6H_6 and CH_3CN) present in the crystal lattice have been omitted for clarity].

ions are 0.73, 0.98, 1.16, and 1.56 nm for L^1 to L^4 ligands, respectively. The Mg ions are perfectly on the least-squares plane of $C_{20}N_4$ porphyrinato core (Table 3) in the molecules.

It is also interesting to obtain an X-ray structure even with a longer ligand spacer such as L^5 to form **1**·L^5 which crystallizes in the monoclinic crystal system. This ligand (L^5) has an extended conformation, and in its complex with Mg(*tn*-OEP), **1**, it holds the two porphyrin frameworks at a Mg···Mg nonbonding distance of 2.01 nm from each other without any marked distortion of the "wheel-and-axle" geometry (Figure 6). Such spacing is already wider than the size of the porphyrin "wheel", which results in an interesting modification of the intermolecular organization. Instead of the most dominant nanowire like architectures observed for **1**·L^1 to **1**·L^4, in which all the porphyrin units are aligned parallel to each other to maintain the offset-stacked overlap, in this structure neighbor-

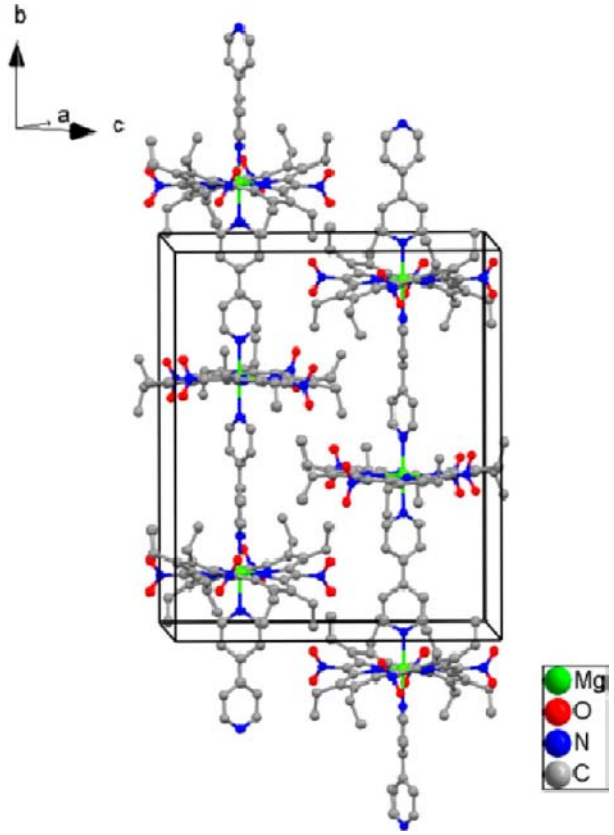

Figure 4. Diagram illustrating the packing of **1**·L^3 in the unit cell at 100 K (H-atoms have been omitted for clarity).

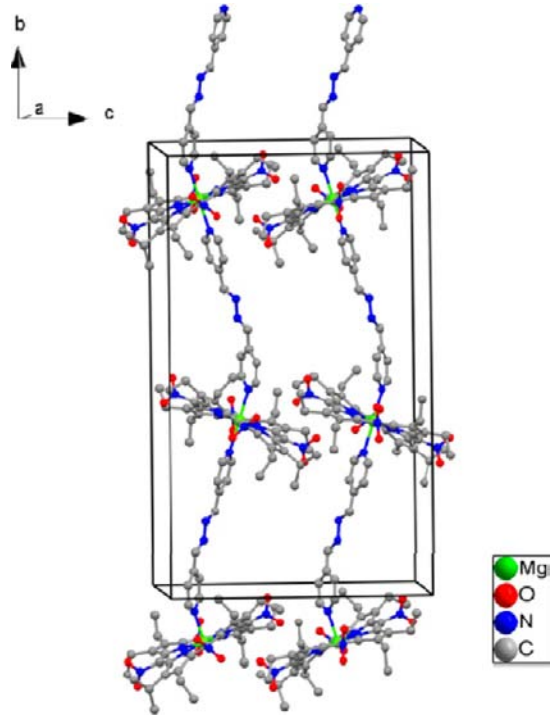

Figure 5. Diagram illustrating the packing of **1**·L^4 in the unit cell at 100 K [H-atoms and the uncoordinated solvent molecules (CH_2Cl_2 and CH_3CN) present in the crystal lattice have been omitted for clarity].

dx.doi.org/10.1021/ic300826p | *Inorg. Chem.* 2012, 51, 9666−9676

Table 1. Crystal Data and Data Collection Parameters

	[1·L^1]·2 L^1	[1·L^2]·C$_6$H$_6$·2CH$_3$CN	1·L^3	[1·L^4]·CH$_2$Cl$_2$·CH$_3$CN	1·L^5
T, K	100(2)	100(2)	100(2)	100(2)	100(2)
formula	$C_{48}H_{52}MgN_{14}O8$	$C_{58}H_{56}MgN_{12}O_8$	$C_{46}H_{48}MgN_{10}O_8$	$C_{101}H_{104}Cl_2Mg_2N_{26}O_{16}$	$C_{90}H_{94}Mg_2N_{22}O_{16}$
formula weight	977.35	1073.46	893.25	2057.62	1788.49
crystal system	orthorhombic	tetragonal	tetragonal	orthorhombic	monoclinic
space group	*Pccn*	*I*4/*mcm*	*I*41/*a*	*Pbca*	*C*2/*c*
a, Å	25.448(4)	16.9582(12)	19.449(5)	18.091(2)	27.248(4)
b, Å	13.497(2)	16.9582(12)	19.449(5)	18.431(2)	15.771(2)
c, Å	14.724(2)	19.600(3)	23.283(5)	30.877(4)	23.201(5)
α, deg	90	90	90	90	90
β, deg	90	90	90	90	115.757(11)
γ, deg	90	90	90	90	90
V, Å^3	5057.3(13)	5636.5(10)	8807(4)	10296(2)	8980(3)
radiation (λ, Å)	Mo Kα (0.71073)	Mo Kα (0.71073)	Mo Kα (0.71073)	Mo Kα (0.71073)	Mo Kα (0.71073)
Z	4	4	8	4	4
d_{calcd} [g cm^{-3}]	1.284	1.265	1.347	1.327	1.323
μ, mm^{-1}	0.102	0.097	0.107	0.153	0.106
F(000)	2056	2256	3760	4312	3760
no. of unique data	4704	1433	4110	9576	8810
no. of params. refined	328	124	298	695	594
GOF on F^2	1.036	1.124	1.030	1.029	1.028
$R1$[a] [$I > 2\sigma(I)$]	0.0751	0.0637	0.0513	0.0735	0.0750
$R1$[a] (all data)	0.1119	0.0724	0.0837	0.1078	0.1352
$wR2$[b] (all data)	0.2102	0.1659	0.1390	0.2113	0.1677

[a] $R1 = \sum||F_o| - |F_c||/\sum|F_o|$. [b] $wR2 = [\sum w(F_o^2 - F_c^2)^2/\sum w(F_o^2)^2]^{1/2}$.

Table 2. Selected Bond Distances (Å) and Angles (deg)

	[1·L^1]·2L^1	[1·L^2]·C$_6$H$_6$·2CH$_3$CN	1·L^3	[1·L^4]·CH$_2$Cl$_2$·CH$_3$CN	1·L^5
			Bond Lengths		
Mg1—N1	2.086(2)	2.082(3)	2.0873(18)	2.093(3)	2.107(3)
Mg1—N2	2.087(2)			2.082(3)	2.088(3)
Mg1—N3				2.087(3)	2.106(3)
Mg1—N4				2.090(3)	2.094(3)
Mg1—N5	2.294(4)	2.237(5)	2.259(3)	2.292(3)	2.138(3)
Mg2—N51			2.1003(19)		
Mg2—N55			2.272(3)		
			Bond Angles		
N1−Mg1—N2	89.96(10)			90.33(11)	88.03(11)
N1−Mg1—N3				178.20(12)	155.48(12)
N1−Mg1—N4				90.07(11)	88.14(11)
N2−Mg1—N3				90.54(11)	87.52(11)
N2−Mg1—N4				178.46(11)	161.93(12)
N3−Mg1—N4				89.10(11)	88.67(11)
N1−Mg1—N5	90.13(7)	90.34(8)	90.19(5)	84.43(10)	101.59(11)
N2−Mg1—N5	89.74(7)			93.25(10)	97.86(11)
N3−Mg1—N5				93.96(10)	102.90(11)
N4−Mg1—N5				88.27(11)	100.21(12)
N51−Mg2—N55			90.89(5)		

ing oligomeric units are arranged in a perpendicular manner and thus fill space more effectively. The linear ligand of the latter is trapped between the concave surfaces of the former, thus yielding a relatively condensed intermolecular arrangement. This arrangement is further facilitated by strong $\pi-\pi$ interactions between the benzene rings of the L^5 ligand with the π-electron cloud of the adjacent porphyrin rings (Figure 6) that are nearly coplanar with interplanar distances varying between 3.50 to 3.65 Å.

In spite of several attempts, we are unable to get X-ray quality crystals of 1·L^6 suitable for structure determinations, but the molecular structures are determined using various spectroscopic techniques and DFT investigations, specifically the Becke[22] three-parameter exchange functional (B3) and the Lee−Yang−Parr correlation functional (LYP).[23] Full geometry optimization has been done for the complex using DFT based on the oligomeric model which, however, ignored the possibility of forming a 1D linear/zigzag coordination polymer. These B3LYP calculations have been carried out with the Gaussian 03, revision B.04, package.[24] Figure 7 shows the optimized molecular structure of the complex in which the Mg···Mg distance has been observed to be 2.70 nm.

dx.doi.org/10.1021/ic300826p | Inorg. Chem. 2012, 51, 9666−9676

Table 3. Selected Structural Parameters for 1·L

compound		Mg–N_p[a]	Mg–N_{ax}[a]	θ[b]	Δ_{24}[c]	$\Delta^{Mg}{}_{24}$[d]	C_m[e]	C_β[f]	Mg···Mg[g]
1·L^1		2.086(2)	2.288(4)	86.4	0.42	0.00	0.06	0.93	0.73
1·L^2		2.082(3)	2.237(5)	90.0	0.40	0.00	0.00	0.89	0.98
1·L^3	core I	2.087(2)	2.259(3)	90.0	0.38	0.00	0.07	0.82	1.16
	core II	2.100(2)	2.272(3)	90.0	0.12	0.00	0.12	0.19	
1·L^4		2.088(3)	2.292(3)	46.2	0.33	0.00	0.02	0.71	1.56
1·L^5		2.099(3)	2.138(3)		0.29	0.44	0.04	0.59	2.01

[a]Average value in Å. [b]Dihedral angle (deg) between two planar pyrazine/pyridine rings of the axial ligands. [c]Average displacement of the 24 atoms (in Å) from the least-squares plane of the porphyrin. [d]Displacement (in Å) of Mg from the least-squares plane of $C_{20}N_4$ pophyrinato core. [e]Average displacement (in Å) of *meso*-carbons from the least-squares plane of $C_{20}N_4$ pophyrinato core. [f]Average displacement (in Å) of *beta*-carbons from the least-squares plane of $C_{20}N_4$ pophyrinato core. [g]The nonbonding distance (in nm) between two adjacent Mg.

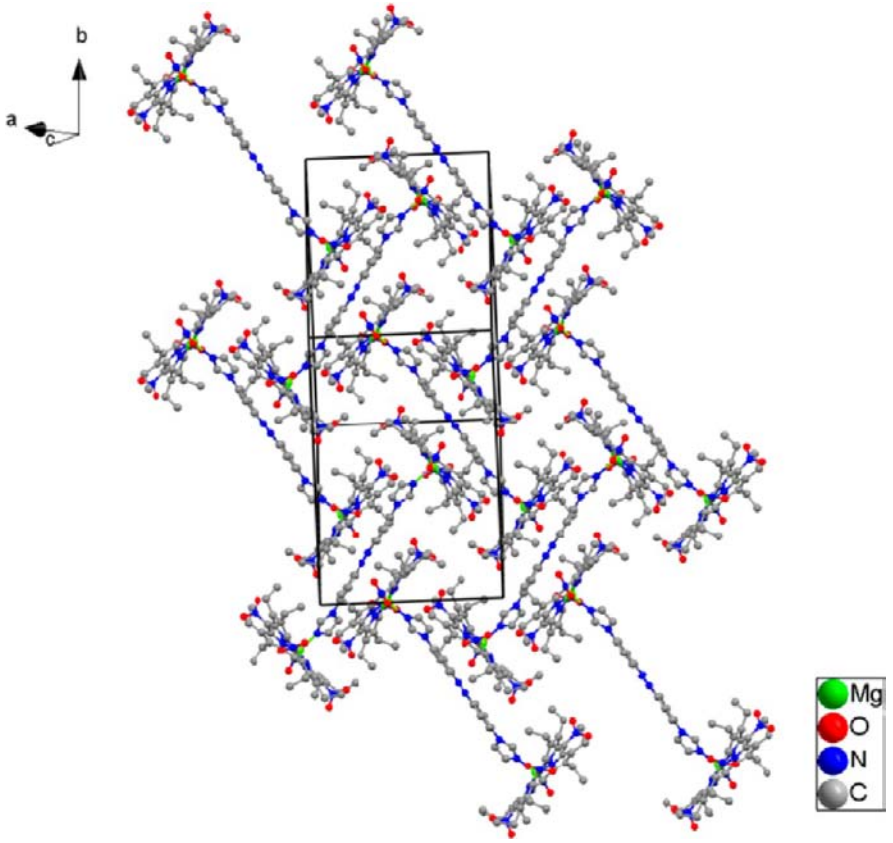

Figure 6. Diagram illustrating the packing of **1**·L^5 in the unit cell at 100 K (H-atoms have been omitted for clarity).

Table 3 compares the key structural features of all the structurally characterized Mg-complexes reported here. Mg is present on the mean porphyrin plane for all the complexes except **1**·L^5 in which the metal is significantly displaced (by 0.44 Å) to produce five-coordinate species. As can be seen, Mg···Mg nonbonding distance increases from 0.73 nm (for **1**·L^1) to 2.01 nm (for **1**·L^5) in the series. The average Mg–N(p) distances varies from 2.082(3) to 2.100(2) Å in the series while the longest distance observed is in **1**·L^5. It is interesting to note the presence of two very different *tn*-OEP cores in **1**·L^3 which include average Mg–N(p), Mg–N(ax) distances and also two crystallographically independent porphyrin rings. The *tn*-OEP rings are highly distorted in all the complexes reported here; however, the distortions are significantly less in **1**·L^5 and in one of the cores in **1**·L^3. Although *tn*-OEP cores are mostly saddle distorted, one of the cores in **1**·L^3 has significant ruffle contributions which accommodates the steric congestion around the periphery; in fact, the distortion observed is lowest among all the complexes reported here and elsewhere[25,26] so far with the same ligand.

The bulk powder samples of the complexes also have the same polymeric structures as observed in the single crystal X-ray structures; Figure 8 and Supporting Information, Figure S1 compare the powder X-ray diffraction (PXRD) pattern of the bulk samples with the simulated pattern obtained from the single crystal X-ray structure for **1**·L^3 and **1**·L^2, respectively, as representative examples.

^{1}H NMR Spectroscopy. ^{1}H NMR experiments were carried out at 295 K in $CDCl_3$ to investigate the structure of the complexes in solution. Figure 9 and Supporting Information, Figure S2 demonstrate the titration of Mg(*tn*-OEP), **1**, with the axial ligands L^1 and L^6, respectively, at 295 K. Trace A of Figure 9 shows the ^{1}H NMR spectrum of Mg(*tn*-OEP) in $CDCl_3$. The protons of free pyrazine (L^1) resonate at 8.58 ppm (trace B) which upon complexation with **1** shifted to the upfield region at 5.31 ppm as demonstrated in trace C. Upfield shifting of the

dx.doi.org/10.1021/ic300826p | *Inorg. Chem.* 2012, 51, 9666–9676

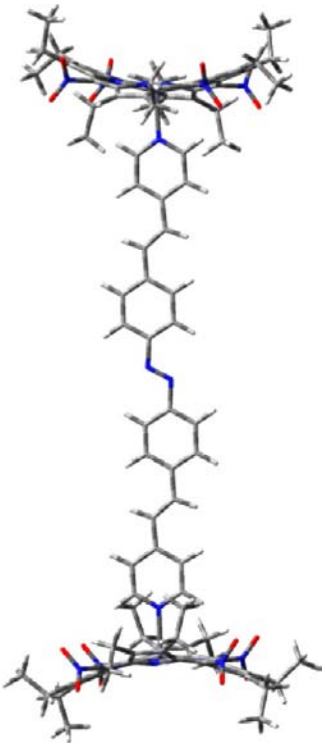

Figure 7. Optimized molecular structure of **1**·L[6] by DFT method at the B3LYP/6-31G** level.

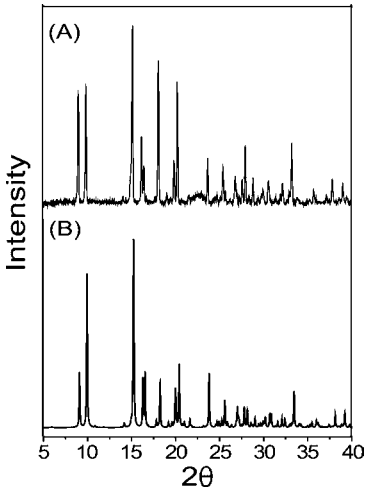

Figure 8. PXRD profiles of **1**·L[3]: (A) bulk powder sample of the complex at 298 K, and (B) simulated pattern obtained from X-ray structure at 100 K.

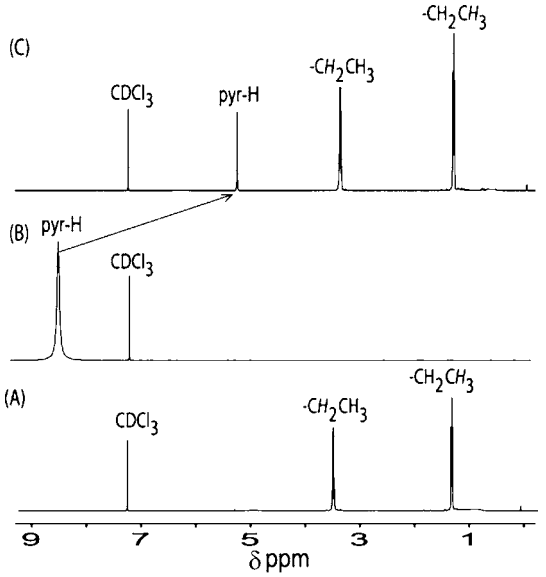

Figure 9. [1]H NMR spectra in $CDCl_3$ (at 295 K) of (A) Mg(*tn*-OEP), **1**, (B) L[1], and (C) **1**·L[1].

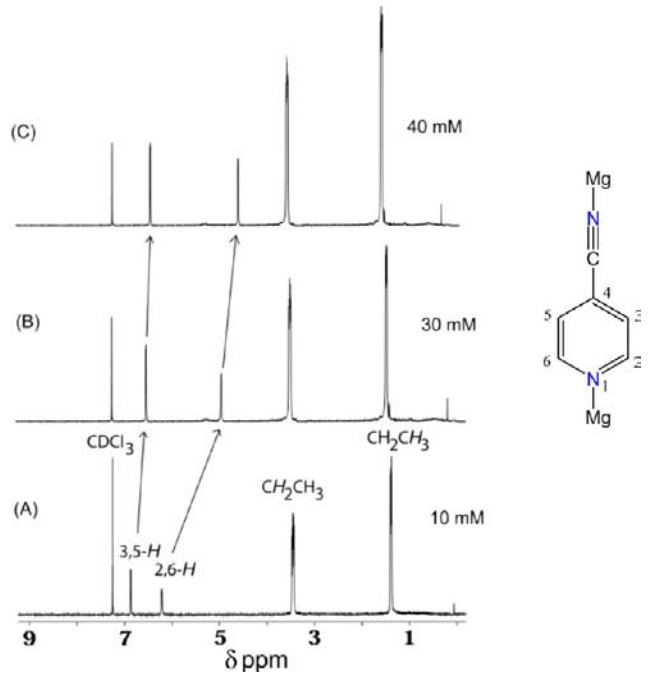

Figure 10. [1]H NMR spectra in $CDCl_3$ (at 295 K) of **1**·L[2] at various concentrations. Inset shows the proton numbering scheme of L[2].

proton resonances of bridging ligand is due to the shielding effect of porphyrin ring current.[27] However, trace C does not display separate peaks because of the coordinated and noncoordinated pyrazine ligand, indicating that they are in fast exchange in the NMR time scale, and thus, the polymeric structure is not stable in solution at 295 K. Upon increasing the concentration, however, the ligand peaks are shifted even more upfield (Figure 10) which indicates the formation of small oligomers in solution. This is due to greater shielding effects experienced by the ligand protons as a result of coordination at the other side. Similar observations arise with other linkers also.

AFM and SEM Images. The morphology of the aggregates formed was examined by Atomic Force Microscopy (AFM) and Scanning Electron Microscopy (SEM) on a freshly cleaved HOPG surface. The complexes were dissolved in tetrahydrofuran (5×10^{-6} M) which were then applied on the HOPG surface by drop deposition method and consequently the self-assembly processes are very stable and reproducible. After immediate evaporation, these films were examined by microscopy; topographic AFM images are shown in Figure 11 while SEM images are shown in Figure 12.

Magnesium in Mg(*tn*-OEP) binds strongly with the conjugated bidentate ligand L which produce long wire-like morphology with several micrometer lengths on the HOPG surface for **1**·L[1] to **1**·L[4] (Figures 11 and 12, traces A-D). From the analysis of the height profile and width (AFM), the

dx.doi.org/10.1021/ic300826p | *Inorg. Chem.* 2012, 51, 9666−9676

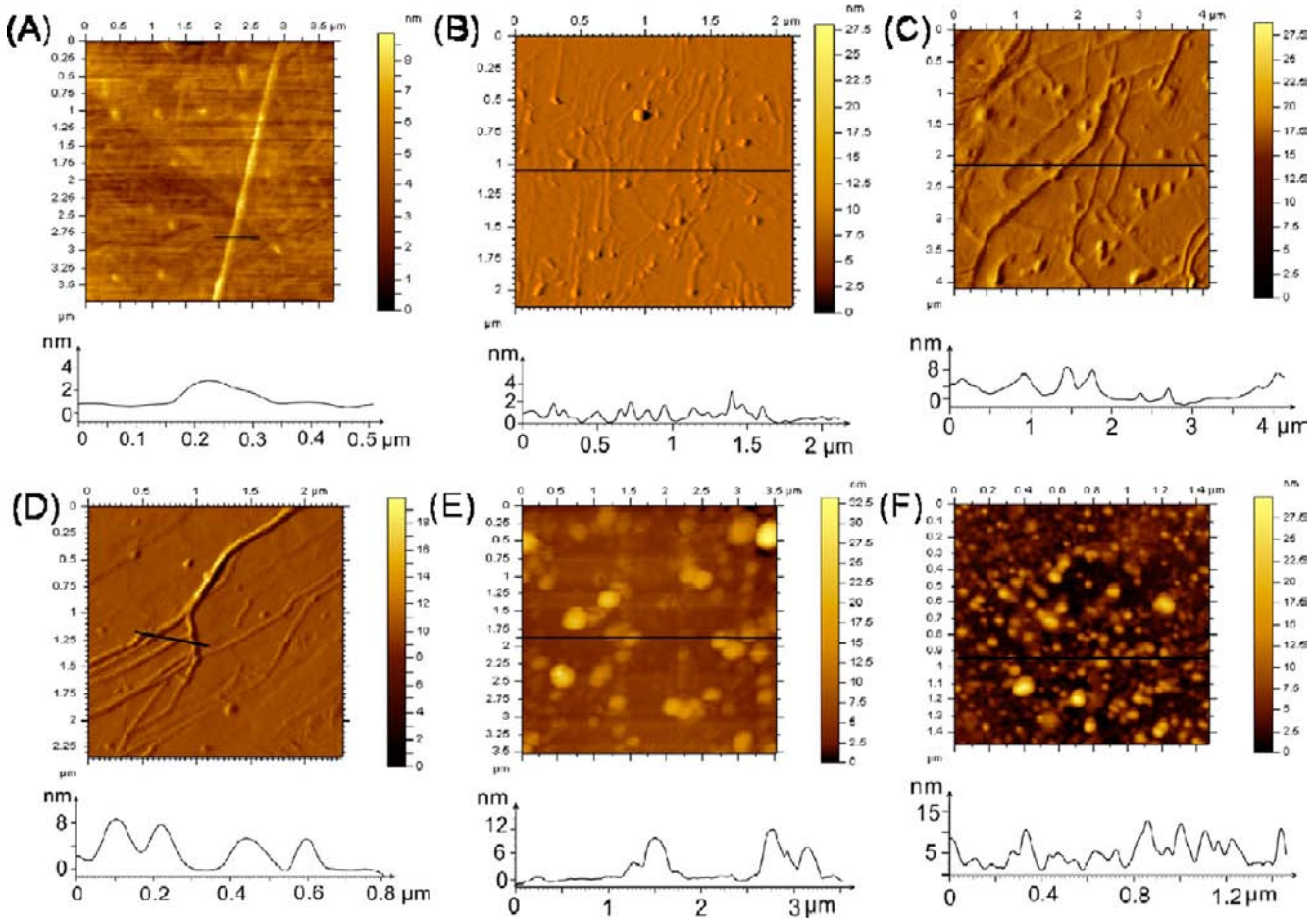

Figure 11. Topographic AFM images of (A) $\mathbf{1}\cdot L^1$, (B) $\mathbf{1}\cdot L^2$, (C) $\mathbf{1}\cdot L^3$, (D) $\mathbf{1}\cdot L^4$, (E) $\mathbf{1}\cdot L^5$, and (F) $\mathbf{1}\cdot L^6$ drop cast onto HOPG from a 5×10^{-6} M solution in tetrahydrofuran. The contours in the frames below the images correspond to the line in the images.

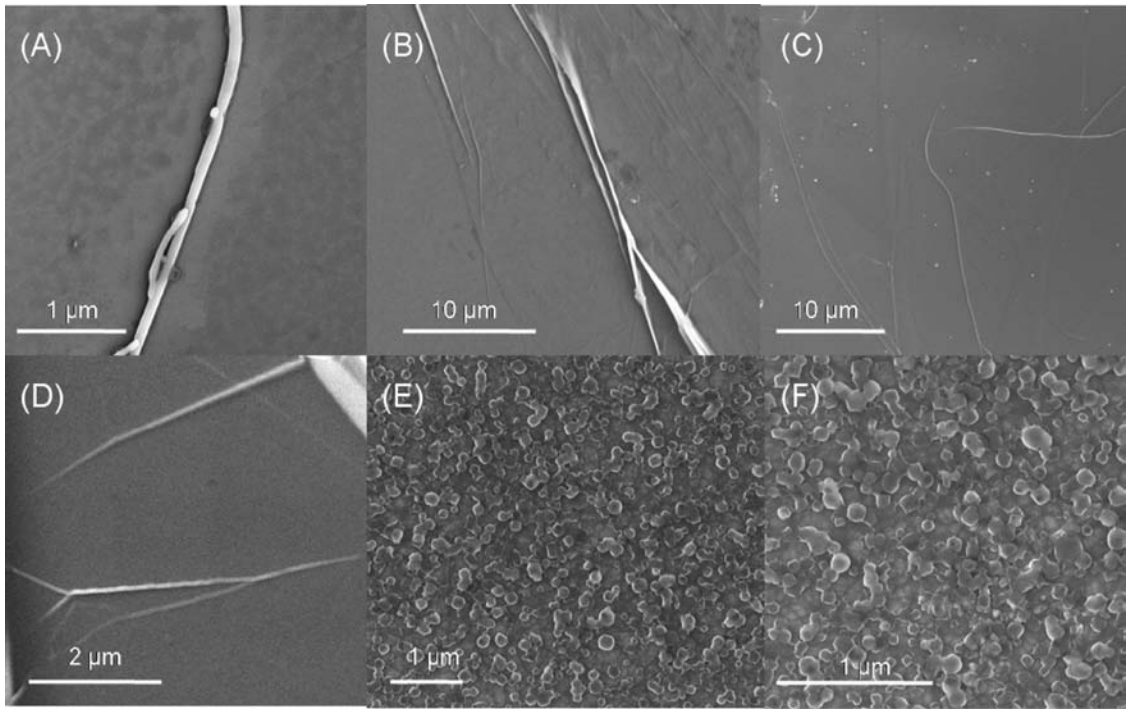

Figure 12. SEM images of (A) $\mathbf{1}\cdot L^1$, (B) $\mathbf{1}\cdot L^2$, (C) $\mathbf{1}\cdot L^3$, (D) $\mathbf{1}\cdot L^4$, (E) $\mathbf{1}\cdot L^5$, and (F) $\mathbf{1}\cdot L^6$ drop cast onto HOPG from 5×10^{-6} M solution in tetrahydrofuran.

dx.doi.org/10.1021/ic300826p | *Inorg. Chem.* 2012, 51, 9666–9676

structures are considered to be side-by-side arrangements of 1D linear chains that have also been observed in the X-ray structure of the molecules. By changing the length of the axial ligand L, the morphology of the supramolecular structures can also be controlled. The minimum height of wires are around 1.5 nm which are about same as the molecular diameter of a 1D chain of porphyrin/bridging ligands.[14f] The lengths of most of the polymeric species are in a range of several micrometers while the widths (AFM) are in the range of 25 to 100 nm. So from these broad width and height profiles, these surface pattern can be considered as side by side aggregations[14b,f,g] of 1D linear chains leading to the formation of rigid and stable 2D arrays which are demonstrated pictorially in Scheme 3. The remarkable length and shape of each wire suggest the rigid nature of the polymer that might be of advantage in future applications.

Scheme 3. Schematic Model of Side by Side Arrangements of 1D Chain

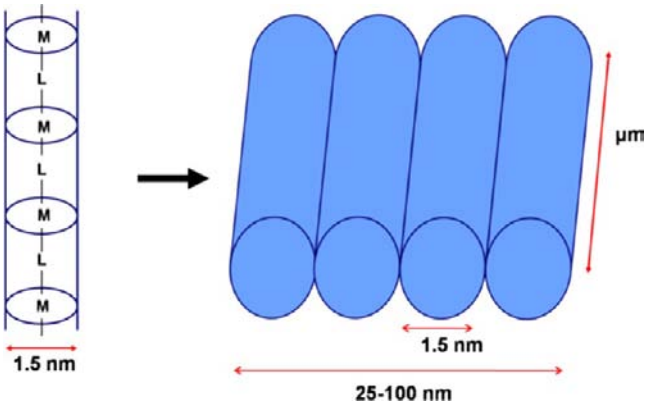

A spherical pattern was found on the HOPG surface for complex **1**·L^5 which had width of 100 to 250 nm and height of around 10 to 15 nm. As observed in the X-ray structure of the complex, the neighboring oligomeric units are oriented in a mutually perpendicular arrangement to optimize $\pi-\pi$ interactions and fill-up effectively the intermolecular space between them. This correlates nicely with the spherical structure observed on the HOPG surface (trace E, Figures 11 and 12). Similar spherical structures were also obtained for **1**·L^6 (trace F, Figures 11 and 12) with width of 50 to 100 nm and a height of around 10 nm. Such assembly appears to be of interest for polymer and macromolecular chemistry where spherical shapes are achieved based on the principle of minimizing the surface area. Spherical assembly is reminiscent of the spherical shape adopted by native chlorophyll *a*.[11e]

CONCLUSIONS

The addition of axial ligand L on Mg(*tn*-OEP), upon spontaneous self-association, readily produces well-defined large-scale aggregates **1**·L in a single pot which precipitate out in pure crystalline form in excellent yields and thus, enable easier isolation of the products. Six conjugated axial ligands L with increasing chain lengths have been utilized in the present investigations. Single crystal X-ray structures of **1**·L^1 to **1**·L^5 have been reported here while full geometrical optimization has been done for **1**·L^6 by DFT. As the length of the bridging ligand increases, the Mg···Mg nonbonding distance between successive magnesium ions also increases from 0.73 to 2.70 nm in the series. To the best of our knowledge, this is the first report where stable Mg-porphyrin with such long spacers (Mg···Mg, 2.70 nm for L^6) has been synthesized in one pot so easily. The present study demonstrates that the addition of four strong electron-withdrawing nitro groups at the *meso* positions in *tn*-OEP have a significant impact on the electronic and structural properties of the Mg-porphyrins, which has significantly enhanced the affinity for axial ligands.

Linear polymeric chains were observed in the X-ray structures of the six-coordinate complexes (**1**·L^1 to **1**·L^4) which form a so-called "shish kebab" like architecture with the bridging bidentate ligand being aligned perpendicularly to the planes of the porphyrin units. Instead of the most dominant nanowire like architectures observed for **1**·L^1 to **1**·L^4, in which porphyrin units are aligned parallel to each other to maintain the offset-stacked overlap, in **1**·L^5 and **1**·L^6 neighboring oligomeric units are arranged in a perpendicular manner forming so-called "wheel-and-axle" like architectures to optimize $\pi-\pi$ interactions and fill-up effectively the intermolecular space between them. This correlates nicely with the spherical structure observed on the HOPG surface.

^{1}H NMR experiments are carried out to investigate the structure of the complexes in solution. Upfield shifting of the proton resonances of bridging ligands are observed because of the shielding effect of the porphyrin ring current which confirms the axial coordination. Monomeric species are mostly present in solution at room temperature.

Long wire-like morphology with several micrometer lengths are observed on the HOPG surface for **1**·L^1 to **1**·L^4. The surface patterns can be considered as side by side arrangements of supramolecular chains leading to the formation of rigid and stable 2D patterns. The lengths of the polymeric species are in a range of several micrometers while widths are in the range of 25 to 100 nm. However, after an optimum Mg···Mg nonbonding distance, these 1D chain do not continue and porphyrin dimers form (in **1**·L^5 and **1**·L^6). These result in spherical structures on the HOPG surface that have widths of 100 to 250 nm and heights of around 10 to 15 nm. Such assembly appears to be of interest for polymer and macromolecular chemistry where spherical shapes are achieved based on the principle of minimizing the surface area.

EXPERIMENTAL SECTION

Materials. The free ligand (*tn*-H_2OEP) was prepared as reported earlier[21a] and the magnesium ion is inserted using a procedure reported previously[21b] for bisporphyrin which produces the previously reported Mg(*tn*-OEP) in excellent yields.[26] Reagents and solvents were purchased from commercial sources and purified by standard procedures before use. The linkers L^1, L^2, and L^3 have been purchased from Sigma-Aldrich while L^4 and L^5 have been synthesized following the reported procedures.[28,29] L^6 is, however, new and synthesized using the procedures stated below.

Synthesis of L^6. 4-Methylpyridine (4 g, 43 mmol) was mixed with 4-nitro benzaldehyde (6.48 g, 43 mmol) in acetic anhydride (40 mL), and the reaction mixture was heated at 145 °C for 8 h. The solution was then cooled slowly to room temperature resulting in a yellow precipitate of the crude product[30] which was collected by filtration and washed well with water, then ethanol, and finally with diethyl ether. The yellow solid (5 g, 24.74 mmol), thus obtained, was dissolved in 2-propanol and heated to reflux to get a clear solution. Aq. NaOH (12 g in 30 mL H_2O) and Zn powder (30 g) were then added one after another to the mixture. The resulting solution was refluxed for 24 h again and then allowed to cool at room temperature. Insoluble materials were removed by filtration, and the filtrate was evaporated to complete dryness, which was extracted with chloroform. The organic

dx.doi.org/10.1021/ic300826p | *Inorg. Chem.* 2012, 51, 9666−9676

layer was washed several times with water, dried over anhydrous Na_2SO_4, and finally evaporated under reduced pressure to obtain an orange solid which was then recrystallized from hexane/chloroform. Yield: 3.86 g (45%). Anal. Calcd (found): C, 80.37 (80.12); H, 5.19 (5.28); N, 14.42 (14.53). ^{1}H NMR (500 MHz, $CDCl_3$, 295 K): δ 8.44 (m, 4H), 8.25 (dd, J = 1.7, 8.6 Hz, 2H), 8.17 (dd, J = 1.8, 8.6 Hz, 2H), 7.60 (m, 4H), 7.37 (m, 4H), 7.32−7.26 (m, 2H), 7.06 (m, 2H). ESI-MS: m/z 389.1764 ($[M+H]^+$).

Complex **1**·L was prepared using the general procedure; details are given below for a representative case.

Synthesis of **1**·L^1. Twenty-five milligrams of **1** (0.03 mmol) was dissolved in 5 mL of dichloromethane. Ten milligrams of pyrazine (0.12 mmol) was added to the solution which was then stirred for 30 min. A greenish precipitation appeared which was then collected by filtration and dried in vacuum. Yield: 21 mg (86%). Anal. Calcd (found): C, 58.80 (58.69); H, 5.43 (5.55); N, 17.15 (17.27). UV−vis (dichloromethane) [λ_{max}, nm (ε, M^{-1} cm^{-1})]: 365 (3.6×10^4), 435 (7.2×10^4), 573 (9.6×10^3), 606 (5.3×10^3). ^{1}H NMR ($CDCl_3$, 295 K): δ 5.31 (s, 4H, Pyr-*H*); 3.43 (q, 16H, $-CH_2CH_3$); 1.41 (t, 24H, $-CH_2CH_3$).

1·L^2. Yield: 22 mg (89%). Anal. Calcd (found): C, 59.97 (59.83); H, 5.27 (5.38); N, 16.66 (16.51). UV−vis (dichloromethane) [λ_{max}, nm (ε, M^{-1} cm^{-1})]: 365 (3.8×10^4), 436 (7.9×10^4), 573 (1.1×10^4), 606 (5.3×10^3). ^{1}H NMR ($CDCl_3$, 295 K): δ 6.86 (br, 2H, 3,5-*H*-4CNPy); 6.06 (br, 2H, 2,6-*H*-4CNPy); 3.43 (q, 16H, $-CH_2CH_3$); 1.41 (t, 24H, $-CH_2CH_3$).

1·L^3. Yield: 23 mg (88%). Anal. Calcd (found): C, 61.85 (61.72); H, 5.42 (5.57); N, 15.69 (15.56). UV−vis (dichloromethane) [λ_{max}, nm (ε, M^{-1} cm^{-1})]: 365 (3.2×10^4), 437 (6.7×10^4), 574 (9.1×10^3), 606 (4.9×10^3). ^{1}H NMR ($CDCl_3$, 295 K): δ 8.46 (br, 4H, 4,4′ bipy); 7.33 (br, 4H, 4,4′ bipy); 3.43 (q, 16H, $-CH_2CH_3$); 1.41 (t, 24H, $-CH_2CH_3$).

1·L^4. Yield: 24 mg (85%). Anal. Calcd (found): C, 60.86 (60.77); H, 5.32 (5.47); N, 17.75 (17.62). UV−vis (dichloromethane) [λ_{max}, nm (ε, M^{-1} cm^{-1})]: 365 (3.6×10^4), 436 (7.05×10^4), 573 (9.5×10^3), 606 (5.1×10^3). ^{1}H NMR ($CDCl_3$, 295 K): δ 8.44 (s, 2H, vinyl-*H*); 8.42 (d, 4H, α-*H*); 7.55 (d, 4H, β-*H*); 3.43 (q, 16H, $-CH_2CH_3$); 1.41 (t, 24H, $-CH_2CH_3$).

1·L^5. Yield: 22 mg (82%). Anal. Calcd (found): C, 60.44 (60.30); H, 5.30 (5.47); N, 17.24 (17.36). UV−vis (dichloromethane) [λ_{max}, nm (ε, M^{-1} cm^{-1})]: 365 (5.2×10^4), 437 (7.6×10^4), 574 (9.7×10^3), 606 (5.1×10^3). ^{1}H NMR ($CDCl_3$, 295 K): δ 7.58 (d, 4H, Ar-*H*); 6.62 (d, 4H, Ar-*H*); 5.65 (s, 2H, Im-*H*); 4.30 (s, 2H, Im-*H*); 2.82 (s, 2H, Im-*H*); 3.43 (q, 16H, $-CH_2CH_3$); 1.41 (t, 24H, $-CH_2CH_3$).

1·L^6. Yield: 23 mg (84%). Anal. Calcd (found): C, 63.20 (63.33); H, 5.41 (5.58); N, 15.05 (15.19). UV−vis (dichloromethane) [λ_{max}, nm (ε, M^{-1} cm^{-1})]: 365 (5.4×10^4), 436 (7.7×10^4), 573 (9.4×10^3), 606 (4.9×10^3). ^{1}H NMR ($CDCl_3$, 295 K): δ 7.98 (d, 2H, Ar-*H*); 7.89 (d, 2H, Ar-*H*); 7.22 (m, 8H, Ar-*H*); 6.64 (m, 2H, Vinyl-*H*); 6.32 (m, 2H, Vinyl-*H*); 6.08 (s, 4H, Ar-*H*); 3.43 (q, 16H, $-CH_2CH_3$); 1.41 (t, 24H, $-CH_2CH_3$).

Instrumentation. UV−vis spectra were recorded on a PerkinElmer UV/vis spectrometer. Elemental (C, H, and N) analyses were performed on a CE-440 elemental analyzer. ^{1}H NMR spectra were recorded on a JEOL 500 MHz instrument. The residual ^{1}H resonances of the solvents were used as a secondary reference. PXRD data were collected on an XPERT-PRO diffractometer using CuKα radiation (λ = 1.540598 Å) at 298 K.

Atomic Force Microscopy. All the samples were imaged using Agilent Technologies Atomic Force Microscopy (AFM) operating under the Acoustic AC mode (AAC), the sample was mounted on the XY stage of the AFM and the integral video camera (NAVITAR, Model N9451A-USO6310233) with the Fiber-lite source, MI-150 high intensity illuminator from Dolan-Jenner Industries was used to isolate the marked regions imbedded with the microscope. Micro fabricated silicon nitride cantilevers (PPP-NCL-20) from Nanosensors. The scanner model N9524A-USO7480132.xml/N9520A-USO7480152.xml was calibrated and used for imaging. The images were taken at room temperature in air with a scan speed of 2.0 lines/sec. Repeated scanning of the sample confirmed that no physical damage occurred during scanning. Data acquisition and analysis was carried out using Pico View 1.8.2. The Images were processed by using Pico Image basic software. Operations such as leveling, filtering, line correction, and form removal were used to process the images for clarity. The image profile was extracted to find the particle size in two dimensions. The third dimension of the particle was determined by its 3D profile. Samples were prepared by placing a drop of the solution on the surface of freshly cleaved HOPG.

Scanning Electron Microscopy. The SUPRA 40VP field emission scanning electron microscope (Carl Zeiss NTS GmbH, Oberkochen, Germany) equipped with energy-dispersive X-ray (EDX), in high vacuum mode operated at 10 kV, was used for the visualization of complexes. Samples were prepared by placing a drop of the solution on the surface of freshly cleaved HOPG which was dried in air and finally under vacuum. Sequential gold sputtering was made before taking an image.

X-ray Structure Solution and Refinement. Crystals were coated with light hydrocarbon oil and mounted in the 100 K dinitrogen stream of Bruker SMART APEX CCD diffractometer equipped with CRYO Industries low-temperature apparatus, and intensity data were collected using graphite-monochromated Mo Kα radiation (λ= 0.71073 Å). The data integration and reduction were processed with the SAINT software.[31] An absorption correction was applied.[32] Structures were solved by the direct method using SHELXS-97 and were refined on F^2 by full-matrix least-squares technique using the SHELXL-97 program package.[33] Non-hydrogen atoms were refined anisotropically. In the refinement, hydrogens were treated as riding atoms using SHELXL default parameters. In **1**·L^2, the axial ligand 4-cyano pyridine (L^2) can coordinate to Mg either through pyridine nitrogen or through the nitrogen of cyano group and thus has orientation disorder. The crystal lattice of **1**·L^5, also contains several severely disordered water molecules which could not be modeled properly because of the weakly diffracting nature of the crystals and thus, the SQUEEZE routine of PLATON was used to remove such uncoordinated and highly disordered water molecules.

Computational Details. DFT calculation have been carried out by employing a B3LYP hybrid functional using the Gaussian 03, revision B.04, package. The method used was Becke's three parameter hybrid exchange functional,[22] the nonlocal correlation provided by the Lee, Yang, and Parr expression, and the Vosko, Wilk, and Nusair 1980 correlation functional (III) for local correction.[23] The basis set was 6-31G** for Mg, C, N, O, and H.

■ ASSOCIATED CONTENT

Ⓢ Supporting Information

PXRD profile of **1**·L^2 (Figure S1), ^{1}H NMR titrations of Mg(*tn*-OEP) with L^6 at 295 K (Figure S2), and X-ray crystallographic details in CIF format. This material is available free of charge via the Internet at http://pubs.acs.org.

■ AUTHOR INFORMATION

Corresponding Author

*E-mail: sprath@iitk.ac.in.

Notes

The authors declare no competing financial interest.

■ ACKNOWLEDGMENTS

We are thankful to the Department of Science and Technology, Government of India and CSIR, India, for financial support. S.A.I. and S.B. thanks CSIR, India, for their fellowships. We are thankful to Prof. M. M. Olmstead of Department of Chemistry, UC Davis, for help with a crystallographic problem.

■ REFERENCES

(1) Liu, C. Y.; Bard, A. J. *Nature* **2002**, *418*, 162−164.
(2) Tsuda, A.; Osuka, A. *Science* **2001**, *293*, 79−82.

(3) (a) Beletskaya, I.; Tyurin, V. S.; Tsivadze, A. Y.; Guilard, R.; Stern, C. *Chem. Rev.* **2009**, *109*, 1659−1713. (b) Aratani, N.; Kim, D.; Osuka, A. *Acc. Chem. Res.* **2009**, *42*, 1922−1934. (c) Maeda, C.; Kamada, T.; Aratani, N.; Osuka, A. *Coord. Chem. Rev.* **2007**, *251*, 2743−2752. (d) Iengo, E.; Zangrando, E.; Alessio, E. *Acc. Chem. Res.* **2006**, *39*, 841−851.

(4) (a) Monti, D.; Nardis, S.; Stefanelli, M.; Paolesse, R.; Natale, C. D.; Amico, A. D. *J. Sensors* **2009**, 1−10. (b) Sanders, J. K. M. In *The Porphyrin Handbook*; Kadish, K. M., Smith, K. M., Guilard, R.; Eds.; Academic Press: New York, 2000; Vol. *3*, pp 347−368.

(5) (a) Michelsen, U.; Hunter, C. A. *Angew. Chem., Int. Ed.* **2000**, *39*, 764−767. (b) Ogawa, K.; Kobuke, Y. *Angew. Chem. Int., Ed.* **2000**, *39*, 4070−4073. (c) Ikeda, C.; Fujiwara, E.; Satake, A.; Kobuke, Y. *Chem. Commun.* **2003**, 616−617. (d) Yoon, D. H.; Lee, S. B.; Yoo, K. H.; Kim, J.; Lim, J. K.; Aratani, N.; Tsuda, A.; Osuka, A.; Kim, D. *J. Am. Chem. Soc.* **2003**, *125*, 11062−11064. (e) Schwab, A. D.; Smith, D. E.; Bond-Watts, B. D.; Johnston, E.; Hone, J.; Johnson, A. T.; dePaula, J. C.; Smith, W. F. *Nano Lett.* **2004**, *4*, 1261−1265. (f) Koepf, M.; Trabolsi, A.; Elhabiri, M.; Wytko, J. A.; Paul, D.; Albrecht-Gary, A. M.; Weiss, J. *Org. Lett.* **2005**, *7*, 1279−1282. (g) Doan, S. C.; Shanmugham, S.; Aston, D. E.; McHale, J. L. *J. Am. Chem. Soc.* **2005**, *127*, 5885−5892. (h) Drobizhev, M.; Stepanenko, Y.; Rebane, A.; Wilson, C. J.; Screen, T. E. O.; Anderson, H. L. *J. Am. Chem. Soc.* **2006**, *128*, 12432−12433. (i) Susumu, K.; Frail, P. R.; Angiolillo, P. J.; Therien, M. J. *J. Am. Chem. Soc.* **2006**, *128*, 8380−8381. (j) Hameren, R. V.; van Buul, A. M.; Castriciano, M. A.; Villari, V.; Micali, N.; Schoen, P.; Speller, S.; Scolaro, L. M.; Rowan, A. E.; Elemans, J. A. A. W.; Nolte, R. J. M. *Nano Lett.* **2008**, *8*, 253−259.

(6) (a) Choi, M. S.; Yamazaki, T.; Yamazaki, I.; Aida, T. *Angew. Chem., Int. Ed.* **2004**, *43*, 150−158. (b) Holten, D.; Bocian, D. F.; Lindsey, J. S. *Acc. Chem. Res.* **2002**, *35*, 57−69. (c) Burrell, A. K.; Officer, D. L.; Plieger, P. G.; Reid, D. C. W. *Chem. Rev.* **2001**, *101*, 2751−2796.

(7) (a) Tanaka, T.; Lee, B. S.; Aratani, N.; Yoon, M. -C.; Kim, D.; Osuka, A. *Chem.—Eur. J.* **2011**, *17*, 14400−14412. (b) Song, J.; Aratani, N.; Kim, P.; Kim, D.; Shinokubo, H.; Osuka, A. *Angew. Chem., Int. Ed.* **2010**, *49*, 3617−3620. (c) Song, J.; Aratani, N.; Shinokubo, H.; Osuka, A. *Chem.—Eur. J.* **2010**, *16*, 13320−13324. (d) Hori, T.; Peng, X.; Aratani, N.; Takagi, A.; Matsumoto, T.; Kawai, T.; Yoon, Z. S.; Yoon, M. -C.; Yang, J.; Kim, D.; Osuka, A. *Chem.—Eur. J.* **2008**, *14*, 582−595. (e) Hori, T.; Aratani, N.; Takagi, A.; Matsumoto, T.; Kawai, T.; Yoon, M. -C.; Yoon, Z. S.; Cho, S.; Kim, D.; Osuka, A. *Chem.—Eur. J.* **2006**, *12*, 1319−1327. (f) Maes, W.; Vanderhaeghen, J.; Smeets, S.; Asokan, C. V.; Renterghem, L. M. V.; Prez, F. E. D.; Smet, M.; Dehaen, W. *J. Org. Chem.* **2006**, *71*, 2987−2994. (g) Aratani, N.; Takagi, A.; Yanagawa, Y.; Matsumoto, T.; Kawai, T.; Yoon, Z. S.; Kim, D.; Osuka, A. *Chem.—Eur. J.* **2005**, *11*, 3389−3404. (h) Choi, M. S.; Aida, T.; Yamazaki, T.; Yamazaki, I. *Angew. Chem., Int. Ed.* **2001**, *40*, 3194−3198.

(8) (a) Satake, A.; Azuma, S.; Kuramochi, Y.; Hirota, S.; Kobuke, Y. *Chem.—Eur. J.* **2011**, *17*, 855−865. (b) Kuramochi, Y.; Sandanayaka, A. S. D.; Satake, A.; Araki, Y.; Ogawa, K.; Ito, O.; Kobuke, Y. *Chem.—Eur. J.* **2009**, *15*, 2317−2327. (c) Kuramochi, Y.; Satake, A.; Itou, M.; Ogawa, K.; Araki, Y.; Ito, O.; Kobuke, Y. *Chem.—Eur. J.* **2008**, *14*, 2827−2841. (d) Dy, J. T.; Ogawa, K.; Satake, A.; Ishizumi, A.; Kobuke, Y. *Chem.—Eur. J.* **2007**, *13*, 3491−3500. (e) Diskin-Posner, Y.; Patra, G. K.; Goldberg, I. *Chem. Commun.* **2002**, 1420−1421. (f) Diskin-Posner, Y.; Patra, G. K.; Goldberg, I. *Dalton Trans.* **2001**, 2775−2782. (g) Kumar, D. K.; Das, A.; Dastidar, P. *Inorg. Chem.* **2007**, *46*, 7351−7361.

(9) (a) Hasobe, T. *Phys. Chem. Chem. Phys.* **2010**, *12*, 44−57. (b) Medforth, C. J.; Wang, Z.; Martin, K. E.; Song, Y.; Jacobsenc, J. L.; Shelnutt, J. A. *Chem. Commun.* **2009**, 7261−7277. (c) Hunter, C. A.; Tomas, S. *J. Am. Chem. Soc.* **2006**, *128*, 8975−8979. (d) Stulz, E.; Scott, S. M.; Ng, Y. -F.; Bond, A. D.; Teat, S. J.; Darling, S. L.; Feeder, N.; Sanders, J. K. M. *Inorg. Chem.* **2003**, *42*, 6564−6574. (e) Aratani, N.; Osuka, A.; Kim, Y. H.; Jeong., D. H.; Kim, D. *Angew. Chem, Int. Ed.* **2000**, *39*, 1458−1462.

(10) Satake, A.; Fujita, M.; Kurimotoa, Y.; Kobuke, Y. *Chem. Commun.* **2009**, 1231−1233.

(11) (a) Jordan, P.; Fromme, P.; Witt, H. T.; Klukas, O.; Saenger, W.; Krauss, N. *Nature* **2001**, *411*, 909−917. (b) McDermott, G.; Prince, S. M.; Freer, A. A.; Lawless, A. M. H.; Papiz, M. Z.; Cogdell, R. J.; Isaacs, N. W. *Nature* **1995**, *374*, 517−521. (c) Deisenhofer, J.; Michel, H. *Science* **1989**, *245*, 1463−1473. (d) Allen, J. P.; Feher, G.; Yeates, T. O.; Rees, D. C.; Deisenhofer, J.; Michel, H.; Huber, R. *Proc. Natl. Acad. Sci. U.S.A.* **1986**, *83*, 8589−8593. (e) Deisenhofer, J.; Epp, O.; Miki, K.; Huber, R.; Michel, H. *Nature* **1985**, *318*, 618−624.

(12) (a) Wang, Z. C.; Medforth, C. J.; Shelnutt, J. A. *J. Am. Chem. Soc.* **2004**, *126*, 15954−15955. (b) Schenning, A. P. H. J.; Benneker, F. B. G.; Geurts, H. P. M. *J. Am. Chem. Soc.* **1996**, *118*, 8549−8552.

(13) (a) Kim, D.; Heo, J.; Ham, S.; Yoo, H.; Lee, C. H.; Yoon, H.; Ryu, D.; Kim, D.; Jang, W. D. *Chem. Commun.* **2011**, *47*, 2405−2407. (b) Gu, Z. Y.; Guo, D. S.; Sun, M.; Liu, Y. *J. Org. Chem.* **2010**, *75*, 3600−3607.

(14) (a) Fathalla, M.; Neuberger, A.; Li, S. C.; Schmehl, R.; Diebold, U.; Jayawickram, J. *J. Am. Chem. Soc.* **2010**, *132*, 9966−9967. (b) Xu, H.; Zheng, J. *Macromol. Chem. Phys.* **2010**, *211*, 2125−2131. (c) Lu, G.; Chen, Y.; Zhang, Y.; Bao, M.; Bian, Y.; Li, X.; Jiang, J. *J. Am. Chem. Soc.* **2008**, *130*, 11623−11630. (d) Gao, Y.; Zhang, X.; Ma, C.; Li, X.; Jiang, J. *J. Am. Chem. Soc.* **2008**, *130*, 17044−17052. (e) Liu, Y.; Ke, C. F.; Zhang, H. Y.; Cui, J.; Ding, F. *J. Am. Chem. Soc.* **2008**, *130*, 600−605. (f) Sato, H.; Tsutsumi, O.; Takeda, K.; Tanaka, H.; Ogawa, T. *Jpn. J. Appl. Phys.* **2006**, *45*, 2324−2327. (g) Liu, Y.; Liang, P.; Chen, Y.; Zhang, Y. M.; Zheng, J. Y.; Yue, H. *Macromolecules* **2005**, *38*, 9095−9099.

(15) Radivojevic, I.; Likhtina, I.; Shi, X.; Singha, S.; Drain, C. M. *Chem. Commun.* **2010**, *46*, 1643−1645.

(16) Jeukens, C. R. L. P. N.; Lensen, M. C.; Wijnen, F. J. P.; Elemans, J. A. A. W.; Christianen, P. C. M.; Rowan, A. E.; Gerritsen, J. W.; Nolte, R. J. M.; Maan, J. C. *Nano Lett.* **2004**, *4*, 1401−1406.

(17) (a) Schwab, A. D.; Smith, D. E.; Bond-Watts, B.; Johnston, D. E.; Hone, J.; Johnson, A. T.; de Paula, J. C.; Smith, W. F. *Nano Lett.* **2004**, *4*, 1261−1265. (b) Schwab, A. D.; Smith, D. E.; Rich, C. S.; Young, E. R.; Smith, W. F.; de Paula, J. C. *J. Phys. Chem. B* **2003**, *107*, 11339−11345.

(18) (a) Kojima, T.; Harada, R.; Nakanishi, T.; Kaneko, K.; Fukuzumi, S. *Chem. Mater.* **2007**, *19*, 51−58. (b) Wang, Z.; Medforth, C. J.; Shelnutt, J. A. *J. Am. Chem. Soc.* **2004**, *126*, 16720−16721.

(19) (a) O'Shea, D. F.; Miller, M. A.; Matsueda, H.; Lindsey, J. S. *Inorg. Chem.* **1996**, *35*, 7325−7338. (b) Lindsey, J. S.; Woodford, J. N. *Inorg. Chem.* **1995**, *34*, 1063−1069.

(20) (a) Kobuke, Y.; Miyaji, H. *Bull. Chem. Soc. Jpn.* **1996**, *69*, 3563−3569. (b) Gerasimchuk, N. N.; Mokhir, A. A.; Rodgers, K. R. *Inorg. Chem.* **1998**, *37*, 5641−5650. (c) Hibbs, W.; Arif, A. M.; Botoshansky, M.; Kaftory, M.; Miller, J. S. *Inorg. Chem.* **2003**, *42*, 2311−2322. (d) Atefi, F.; Mcmurtrie., J. C.; Arnold, D. P. *Dalton Trans.* **2007**, 2163−2170. (e) Bhuyan, J.; Sarkar, S. *Cryst. Growth Des.* **2011**, *11*, 5410−5414.

(21) (a) Gong, L.; Dolphin, D. *Can. J. Chem.* **1985**, *63*, 401−405. (b) Lintuluoto, J. M.; Borovkov, V. V.; Inoue, Y. *J. Am. Chem. Soc.* **2002**, *124*, 13676−13677.

(22) Becke, A. D. *J. Chem. Phys.* **1993**, *98*, 5648−5652.

(23) Lee, C.; Yang, W.; Parr, R. G. *Phys. Rev. B.* **1988**, *37*, 785−789.

(24) Frisch, M. J.; Trucks, G. W.; Schlegel, H. B.; Scuseria, G. E.; Robb, M. A.; Cheeseman, J. R.; Montgomery, J. A. Jr.; Vreven, T.; Kudin, K. N.; Burant, J. C.; Millam, J. M.; Iyengar, S. S.; Tomasi, J.; Barone, V.; Mennucci, B.; Cossi, M.; Scalmani, G.; Rega, N.; Petersson, G. A.; Nakatsuji, H.; Hada, M.; Ehara, M.; Toyota, K.; Fukuda, R.; Hasegawa, J.; Ishida, M.; Nakajima, T.; Honda, Y.; Kitao, O.; Nakai, H.; Klene, M.; Li, X.; Knox, J. E.; Hratchian, H. P.; Cross, J. B.; Bakken, V.; Adamo, C.; Jaramillo, J.; Gomperts, R.; Stratmann, R. E.; Yazyev, O.; Austin, A. J.; Cammi, R.; Pomelli, C.; Ochterski, J. W.; Ayala, P. Y.; Morokuma, K.; Voth, G. A.; Salvador, P.; Dannenberg, J. J.; Zakrzewski, V. G.; Dapprich, S.; Daniels, A. D.; Strain, M. C.; Farkas, O. ; Malick, D. K.; Rabuck, A. D.; Raghavachari, K.; Foresman,

J. B.; Ortiz, J. V.; Cui, Q.; Baboul, A. G.; Clifford, S.; Cioslowski, J.; Stefanov, B. B.; Liu, G.; Liashenko, A.; Piskorz, P.; Komaromi, L.; Martin, R. L.; Fox, D. J.; Keith, T.; Al-Laham, M. A.; Peng, C. Y.; Nanayakkara, A.; Challacombe, M.; Gill, P. M. W.; Johnson, B.; Chen, W.; Wong, M. W.; Gonzalez, C.; Pople, J. A. *Gaussian 03*, revision B.04; Gaussian, Inc.: Pittsburgh, PA, 2003.

(25) (a) Patra, R.; Chaudhury, A.; Ghosh, S. K.; Rath, S. P. *Inorg. Chem.* **2008**, *47*, 8324−8335. (b) Ghosh, S. K.; Patra, R.; Rath, S. P. *Inorg. Chem.* **2008**, *47*, 9848−9856. (c) Patra, R.; Rath, S. P. *Inorg. Chem. Commun.* **2009**, 515−519. (d) Patra, R.; Bhowmik, S.; Ghosh, S. K.; Rath, S. P. *Eur. J. Inorg. Chem.* **2009**, 654−665. (e) Patra, R.; Chaudhury, A.; Ghosh, S. K.; Rath, S. P. *Inorg. Chem.* **2010**, *49*, 2057−2067. (f) Patra, R.; Bhowmik, S.; Ghosh, S. K.; Rath, S. P. *Dalton. Trans.* **2010**, *39*, 5795−5806. (g) Chaudhury, A.; Patra, R.; Rath, S. P. *Indian J. Chem.* **2011**, *50A*, 432−437.

(26) Senge, M. O. *J. Porphyrins Phthalocyanines* **1998**, *2*, 107−121.

(27) (a) Davidson, G. J. E.; Lane, L. A.; Raithby, P. R.; Warren, J. E.; Robinson, C. V.; Sanders, J. K. M. *Inorg. Chem.* **2008**, *47*, 8721−8726. (b) Plieger, P.; Burrell, A. K.; Hall, S. B.; Officer, D. L. *J. Inclusion Phenom. Macrocyclic Chem.* **2005**, *53*, 143−148. (c) Twyman, L. J.; King, A. S. H. *Chem. Commun.* **2002**, 910−911.

(28) Kennedy, A. R.; Brown, K. G.; Graham, D.; Kirkhouse, J. B.; Kittner, M.; Major, C.; Mchugh, C. J.; Murdoch, P.; Smith, W. E. *New J. Chem.* **2005**, *29*, 826−832.

(29) Sharma, M. K.; Bharadwaj, P. K. *Inorg. Chem.* **2011**, *50*, 1889−1897.

(30) Lorance, E. D.; Kramer, W. H.; Gould, I. R. *J. Am. Chem. Soc.* **2002**, *124*, 15225−15238.

(31) *SAINT+*, 6.02 ed.; Bruker AXS: Madison, WI, 1999.

(32) Sheldrick, G. M. *SADABS* 2.0; University of Göttingen: Göttingen, Germany, 2000.

(33) Sheldrick, G. M. *Acta Crystallogr.* **2008**, *A64*, 112.